

Incoherent transport in a model for the strange metal phase: Memory-matrix formalism

Emile Pangburn,¹ Anurag Banerjee,² Hermann Freire,³ and Catherine Pépin¹

¹*Institut de Physique Théorique, Université Paris-Saclay, CEA, CNRS, F-91191 Gif-sur-Yvette, France*

²*Department of Physics, Ben-Gurion University of the Negev, Beer-Sheva 84105, Israel*

³*Instituto de Física, Universidade Federal de Goiás, 74.001-970, Goiânia-GO, Brazil*

We revisit a phenomenological model of fermions coupled to fluctuating bosons that emerges from finite-momentum particle-particle pairs for describing the strange metal phase in the cuprates. The incoherent bosons dominate the transport properties for the resistivity and optical conductivity in the non-Fermi liquid phase. Within the Kubo formalism, the resistivity is approximately linear in temperature with a Drude form for the optical conductivity, such that the Drude lifetime is inversely proportional to the temperature. Here, we compute the transport properties of such bosons within the memory-matrix approach that successfully captures the hydrodynamic regime. This technique emerges as the appropriate framework for describing the transport coefficients of the strange metal phase. Our analysis confirms the T -linear resistivity due to the Umklapp scattering that we obtained for this effective model. Finally, we provide new predictions regarding the variation of the thermal conductivity with temperature and examine the validity of the Wiedemann-Franz law.

I. INTRODUCTION

One of the most enduring mysteries of quantum condensed matter physics is arguably the strange metal phase of the cuprate superconductors [1–3]. The conventional metal obeys universal laws for the variation of transport coefficients with temperature. The standard transport theory of metals gives a simple dependence of the longitudinal σ_{xx} and Hall σ_{xy} conductivities as a function of transport lifetime with $\sigma_{xx} = ne^2\tau/m$ and $\sigma_{xy} = ne^3B\tau^2/c$, where n is the number of electrons, e is the elementary charge, τ is their lifetime, m is their mass, B is the magnetic field and c is the speed of light. At low temperatures, the inverse of the transport time typically goes like $\tau^{-1} \sim T^2$; hence, the longitudinal conductivity displays $\sigma_{xx} \sim T^{-2}$, whereas the Hall conductivity is given by $\sigma_{xy} \sim T^{-4}$. Within the Fermi liquid theory, which describes the behavior of conventional metals, electronic quasiparticles are the sole type of charge carriers and, therefore, the Hall angle becomes $\cot \theta_H = \sigma_{xx}/\sigma_{xy} \sim T^2$.

By contrast, the experimental data in the strange metal phase of the cuprates display striking discrepancies with the standard Fermi liquid picture [4–6]. Firstly, the experimental observations demonstrate that $\sigma_{xx} \sim T^{-1}$ [7] and, at the same time, $\cot \theta_H \sim T^2$ [8–10]. Therefore, the transport time induced from the longitudinal conductivity scales as $\tau \sim T^{-1}$, while the “Hall lifetime” varies as $\tau_H \sim T^{-2}$, which is commonly referred to as the “separation of lifetimes” in the literature [11–13]. Furthermore, the Wiedemann-Franz law is satisfied (with a doping-dependent overall coefficient) in the strange metal phase almost down to $T = 0$ [14–16]. The notable disagreement between the different experimental data with the Fermi-liquid paradigm makes the strange metal phase of the cuprates one of the biggest enigmas of correlated quantum matter [1, 12, 17–19].

The theoretical concepts which have been put forward to explain this very unusual situation can be summarized as follows. Quantum critical theories based on fermions interacting with Landau-damped critical bosons have been widely studied [20]. In these scenarios, electric charge is solely carried by the fermions. From this perspective, two cases emerge.

First, suppose the bosons have finite momentum like in the antiferromagnetic quantum critical theory, among others. In that case, the fermions around the Fermi surface are partially sensitive to the scattering via the bosons. The proportion of the fermions that participate in such scattering is called “hot” fermions, and the remaining part of the Fermi surface remains insensitive to the critical bosons. Since the latter fermions do not participate in the scattering, they are referred to as “cold” fermions. This scenario was first identified in a seminal paper by Hlubina and Rice [21]. This mechanism is the principal obstacle to obtaining a linear-in- T resistivity in these models within the clean limit. Indeed, at low enough temperatures, the “cold” fermions short-circuit the “hot” ones, and the transport lifetime falls back into the standard Fermi liquid paradigm with $\tau^{-1} \sim T^2$ (see also Ref. [22] for an example of this mechanism at play in the context of such systems with the subsequent addition of disorder).

The second possibility within the fermion-boson quantum critical scenario is that the whole Fermi surface becomes “hot”, namely, that the critical bosons have zero momentum so that every fermion at the Fermi surface can participate in the scattering via the bosons (like in the Ising-nematic quantum critical theory, among others). Here all the fermions are “hot”; there is no issue with a possible “short-circuiting” with cold species. A caveat with this scenario is that a T -linear resistivity needs to be clearly obtained within the clean limit, with the temperature dependence of the resistivity varying from sublinear at high temperatures to quadratic at low enough temperatures [23]. Altogether, accounting for such a linear-in- T resistivity with only fermions as charge carriers is challenging. New proposals then emerged, introducing new strongly coupled fixed point models within the Planckian limit of dissipation [19]. These very innovative scenarios (e.g., [17]) have in common that charge carriers are not well-defined and that the systems are analogous to a highly-correlated plasma carrying the current. Strongly correlated fixed point models, including, e.g., the Sachdev-Ye-Kitaev (SYK) model (see [24]), obtain the linear-in- T behavior in the resistivity very elegantly. However, it is not clear yet how to deal with the “two-lifetime” problem within such a scenario. Also, the discussion of the fundamental Planckian limit in these models led to interest-

ing holographic descriptions using hydrodynamic modes and symmetries (see, e.g., [25]).

In the present manuscript, we address such a longstanding issue by proposing a new type of bosonic excitation that can potentially describe the strange metal phase in the cuprates [10, 26–31]. We would like to stress that the scenario explored below presents a unique case where the whole picture, including linear-in- T resistivity and the cotangent of the Hall angle, is addressed, and contact with experiments is made possible. The physical picture underlying our phenomenological model [32, 33] can be summarized as follows: At high energies, the microscopic lattice model generates fluctuating finite momenta bosons created from particle-particle pairs (remnants of a pair-density-wave) and the constituent fermions. These fluctuating bosons carry an electric charge of $2e$ and, hence, also contribute to the charge transport. Moreover, due to the scattering with fermions, such bosons become incoherent as the bosonic propagator becomes $D^{-1}(\mathbf{q}, \omega) = -i\omega + \mathbf{q}^2 + m_b(T)$ (where $m_b(T)$ is the temperature-dependent bosonic mass). Such bosons in two dimensions indeed lead to a T -linear contribution to the longitudinal conductivity and also the optical conductivity attains a Drude form $\sigma_{xx}^{\text{boson}}(\omega) \sim (\tau_{\text{boson}}^{-1} - i\omega)^{-1}$, as shown in Ref. [32]. Interestingly, recent study [34] reveals a bosonic strange metal phase in nanopatterned YBCO samples. In that work, the longitudinal conductivity shows a linear temperature and field dependence along with a vanishing Hall coefficient, as soon as the bosonic transport sets in [34]. Moreover, we also point out the Ref. [26], where another charged carrier is suggested besides the fermions. This additional charge carrier has the experimental signature of contributing to the linear-in- T behavior in the longitudinal resistivity, whereas it does not contribute to the Hall conductivity.

Indeed, since the critical bosons turn out to be particle-hole symmetric, they do not contribute to the transverse Hall conductivity $\sigma_{xy}^{\text{boson}} = 0$. Such a general picture could explain the experimental data if the bosons are light enough to short-circuit the fermions for the longitudinal conductivity. Since the fermions are also present in this model, there must be scattering between these two excitations. As stated above, at low temperatures, scattering via incoherent bosons with finite momentum produces a finite lifetime for the fermions, at least on parts of the Fermi surface, with the generation of “hot spots” where the dominant scattering is through the incoherent bosons, leading to a scattering rate $\tau_{\text{hot}}^{-1} \sim T^\alpha$, with $1 < \alpha < 1.5$ [21, 22]. As explained before, the part of the Fermi surface which is unaffected by the boson scattering is called “cold”. The modeling of the Hall conductivity on a Fermi surface with an anisotropic lifetime has been treated in another study to describe the strange metal phase of the cuprates [35]. The angular average on the Fermi surface favors [35] the “hot regions” for the Hall conductivity, leading to an average Hall inverse lifetime $\tau_H^{-1} \sim T^{3/2}$. Our study thus combines the two types of excitations (bosons and fermions) to give a new perspective to the old paradox, such that the Hall angle becomes $\cot \theta_H \sim T^3/T \sim T^2$, consistent with the experiments.

Since the model of fermion-boson “soup” with charged-two

bosons is one of the few proposals for a regime with linear-in- T resistivity and $\cot \theta_H \sim T^2$, and considering the very scarce number of studies of transport due to charged bosons, it is important to check the universality of this regime and to use another approach to calculate transport properties instead of the Kubo formula implemented in Ref. [32]. In the present paper, we revisit this problem in the context of the hydrodynamic description used in the discussion of the Planckian regime [25, 36] and confirm our key results that such charge-two incoherent bosons in two dimensions contribute to the longitudinal conductivity as $\sigma_{xx} \sim T^{-1}$. To this end, we investigate the transport properties of such bosons using the memory-matrix technique, that successfully captures the hydrodynamic regime. Consequently, the T -linear resistivity regime of the Landau-damped charged bosons with finite momentum due to Umklapp interactions stands on firm ground. Finally, we provide new predictions regarding thermal conductivity as a function of temperature in the model and also discuss the validity of the Wiedemann-Franz law for this system.

II. THE MODEL

We consider here a two-dimensional phenomenological model [32] of fluctuating charge-two bosons interacting with each other and among themselves. The bosons are in a “soup” of fermions, and the corresponding fermion-boson scattering affects the boson lifetime significantly (to be explained below). The bosonic part of the Hamiltonian is given by

$$\hat{H} = \sum_{\mathbf{q}} b_{\mathbf{q}}^{\dagger} \left[\frac{|\mathbf{q}|^2}{2m_b} + \mu_0 \right] b_{\mathbf{q}} + \frac{\lambda^2}{2N} \sum_{\mathbf{q}} \mathcal{Q}_{\mathbf{q}} \mathcal{Q}_{-\mathbf{q}}, \quad (1)$$

where μ_0 and λ denote, respectively, the bare bosonic mass term and the boson-boson interaction, and $\mathcal{Q}_{\mathbf{q}} = \sum_{\mathbf{k}} b_{\mathbf{k}+\mathbf{q}}^{\dagger} b_{\mathbf{k}}$, where $b_{\mathbf{k}}^{\dagger}$ ($b_{\mathbf{k}}$) is the creation (annihilation) operator for a boson with momentum \mathbf{k} . The flavor indices are suppressed to not clutter up the notation. Although the spin index is not shown for simplicity, we allow for the possibility that the bosons have either spin-zero or spin-one. As mentioned above, the model also possesses a “background” of fermions (not shown in the Hamiltonian of Eq. (1)) and the corresponding fermion-boson scattering processes lead to retardation effects, which are taken into account via the one-loop bosonic self-energy $\Sigma(\omega) = -i\gamma\omega$, where the Landau-damping constant γ is given by $\gamma = g_I^2 \mathcal{N}(\epsilon_F) / (2\pi \sqrt{(2k_F Q_0)^2 - Q_0^4})$, with $\mathcal{N}(\epsilon_F)$ being the density of states at the Fermi energy, k_F is the corresponding Fermi momentum, Q_0 is the finite momentum of the bosons and g_I is the fermion-boson interaction. In a previous work [32], we have demonstrated using the Kubo formula that this effective model indeed displays a quantum critical phase with approximately T -linear resistivity and shows a Drude form for the optical conductivity.

We now proceed to calculate the transport properties of this effective model within the memory-matrix (MM) formalism [37–39] (for more information about the technicalities of this

method, see, e.g., Refs. [17, 23, 36, 40–52]). The MM approach emerges as a more suitable framework to describe the non-Fermi liquid phase exhibited, since (i) it does not rely on the existence of well-defined quasiparticles at low energies, and (ii) it successfully captures the hydrodynamic regime that is expected to describe the non-equilibrium dynamics of this strongly correlated metallic phase.

Here, we will follow an approach similar to that used in the recent work by Wang and Berg [23] to calculate transport properties in the context of an Ising-nematic quantum critical theory. In this way, we will project the non-equilibrium dynamics of the present model in terms of slowly-varying operators that are nearly conserved. Naturally, the boson operators $n_{\mathbf{k}} = b_{\mathbf{k}}^\dagger b_{\mathbf{k}}$ turn out to be nearly conserved in the limit of either small λ or large N , since the equation of motion for these operators is given by

$$\begin{aligned} \dot{n}_{\mathbf{k}} &= i \left[\hat{\mathcal{H}}, n_{\mathbf{k}} \right] \\ &= \frac{2\lambda^2 i}{N} \sum_{\mathbf{q}} \mathcal{Q}_{-\mathbf{q}} \left(b_{\mathbf{k}+\mathbf{q}}^\dagger b_{\mathbf{k}} - b_{\mathbf{k}}^\dagger b_{\mathbf{k}-\mathbf{q}} \right) - h.c.. \end{aligned} \quad (2)$$

In the MM formalism, to leading order in $1/N$, the memory matrix writes

$$M_{\mathbf{k}\mathbf{k}'}(\Omega) = \frac{1}{i\Omega} \left[G_{\dot{n}_{\mathbf{k}}\dot{n}_{\mathbf{k}'}}^R(\Omega) - G_{\dot{n}_{\mathbf{k}}\dot{n}_{\mathbf{k}'}}^R(0) \right], \quad (3)$$

where $G_{AB}^R(\Omega)$ is the retarded Green's function for nearly-conserved operators A and B , which is calculated to zeroth order in $1/N$. The MM turns out to be a generalization of the quasiparticle scattering rate in Boltzmann theory (but applicable also to non-Fermi liquids in which this latter quantity cannot be defined) and enters as a retardation process in the calculation of the optical conductivity $\sigma(\Omega)$ and the thermal conductivity at zero electric field $\bar{\kappa}(\Omega)$ in the following way

$$\sigma(\Omega) = \sum_{\mathbf{k}\mathbf{k}'} \chi_{J_{\mathbf{k}}n_{\mathbf{k}}} \left(\frac{1}{M_{\mathbf{k}\mathbf{k}'}(\Omega) - i\Omega\chi_{\mathbf{k}\mathbf{k}'}} \right) \chi_{J_{\mathbf{k}'}n_{\mathbf{k}'}} \quad (4)$$

$$\bar{\kappa}(\Omega) = \frac{1}{T} \sum_{\mathbf{k}\mathbf{k}'} \chi_{J_{\mathbf{k}}^{\mathcal{Q}}n_{\mathbf{k}}} \left(\frac{1}{M_{\mathbf{k}\mathbf{k}'}(\Omega) - i\Omega\chi_{\mathbf{k}\mathbf{k}'}} \right) \chi_{J_{\mathbf{k}'}^{\mathcal{Q}}n_{\mathbf{k}'}} \quad (5)$$

where $J_{\mathbf{k}}$ and $J_{\mathbf{k}}^{\mathcal{Q}}$ are, respectively, the electric current and the thermal current operators of the model, with the corresponding susceptibilities given by $\chi_{J_{\mathbf{k}}n_{\mathbf{k}}} = \int_0^\beta d\tau \langle J_{\mathbf{k}}(\tau) n_{\mathbf{k}}(0) \rangle$, $\chi_{\mathbf{k}\mathbf{k}'} = \int_0^\beta d\tau [\langle n_{\mathbf{k}}(\tau) n_{\mathbf{k}'}(0) \rangle - \langle n_{\mathbf{k}} \rangle \langle n_{\mathbf{k}'} \rangle]$, and $\chi_{J_{\mathbf{k}}^{\mathcal{Q}}n_{\mathbf{k}}} = \int_0^\beta d\tau \langle J_{\mathbf{k}}^{\mathcal{Q}}(\tau) n_{\mathbf{k}}(0) \rangle$.

We point out that the thermal conductivity at zero electric current of the model (which will be denoted here by κ) is given by $\kappa = \bar{\kappa} - T\alpha^2/\sigma$, where α is the thermoelectric coefficient. Since we have demonstrated in a previous work [32] that the present model has particle-hole symmetry, the critical contribution to the thermoelectric response is expected to vanish. Therefore, in this case, the thermal conductivity at zero electric current will be equal to the thermal conductivity at zero electric field (i.e., $\kappa = \bar{\kappa}$).

Furthermore, for clean systems, if no coupling to the lattice is present, the memory matrix of the model also vanishes identically (see Appendix A). However, if Umklapp terms are taken into account, we get after contracting the vertices the following result:

$$M_{\mathbf{k}\mathbf{k}'}(\Omega) = 8\delta_{\mathbf{k}\mathbf{k}'} \sum_{\mathbf{p},\mathbf{q}} \mathcal{M}_{\mathbf{k},\mathbf{p},\mathbf{q}}, \quad (6)$$

with the corresponding Feynman diagram given by Fig. 1.

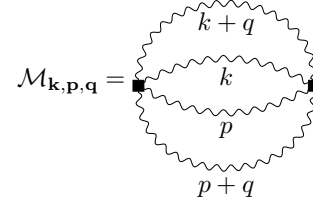


FIG. 1. The Feynman diagram for the calculation of the memory matrix $\mathcal{M}_{\mathbf{k},\mathbf{p},\mathbf{q}}$ showing up in Eq. (6) of the present model. The wavy lines are the boson propagator defined in Eq. (7). The summation is over the momenta \mathbf{p} and \mathbf{q} .

III. RESULTS

A. Evaluations

We now compute the various terms in Eqs. (4) and (5) within our MM formalism. For convenience, we use units such that $e = k_B = \hbar = 1$ from now on. We start from the renormalized propagator for the incoherent bosons given by

$$D_{\mathbf{k}}^{-1} = |\omega_n| + \mu_k(T), \quad (7)$$

with $\mu_k(T) = k^2 + \frac{\lambda^2}{2N}T$. The damping term $|\omega_n|$ (we have set $\gamma = 1$) comes from the scattering via fermionic carriers, and it is responsible for the incoherent character of the bosons. The potential μ_k has a term k^2 , which refers to the bosonic dispersion. Note that the bosons have a mass scaling with temperature (the T term in μ_k). It comes mainly from the Hartree diagram generated by the four-boson interaction.

We begin with the evaluation of

$$\chi_{J_{\mathbf{k}}n_{\mathbf{k}}} = v_{\mathbf{k}} \int_0^\beta d\tau \langle n_{\mathbf{k}}(\tau) \rangle \langle n_{\mathbf{k}}(0) \rangle + v_{\mathbf{k}}\chi_{\mathbf{k}\mathbf{k}}, \quad (8)$$

with $v_{\mathbf{k}} = \mathbf{k}/m_b$. Henceforth, we define

$$\chi_{J_{\mathbf{k}}n_{\mathbf{k}}}^{(a)} = v_{\mathbf{k}} \int_0^\beta d\tau \langle n_{\mathbf{k}}(\tau) \rangle \langle n_{\mathbf{k}}(0) \rangle, \quad (9)$$

$$\chi_{J_{\mathbf{k}}n_{\mathbf{k}}}^{(b)} = v_{\mathbf{k}}\chi_{\mathbf{k}\mathbf{k}}. \quad (10)$$

The first term in Eq. (8) can be found to be equal to (see Appendix B 1)

$$\chi_{J_{\mathbf{k}}n_{\mathbf{k}}}^{(a)} = \frac{v_{\mathbf{k}}n_B(\mu_k)}{\pi} \ln \left(\frac{D}{\mu_k} \right), \quad (11)$$

where D is the bandwidth of the boson dispersion and n_B is the Bose-Einstein distribution. Regarding the second term in Eq. (8), we use the generalized susceptibility $\chi_{\mathbf{k}\mathbf{k}'} = \delta_{\mathbf{k}\mathbf{k}'} T \sum_{\omega_n} D_{\mathbf{k}}^2$, which gives (see Appendix B 1)

$$\chi_{\mathbf{k}\mathbf{k}'} = \delta_{\mathbf{k}\mathbf{k}'} \frac{T}{\mu_k^2} \left(\tanh^{-1} \frac{T}{\mu_k} \right)^2. \quad (12)$$

The analytical formula of Eq. (12) has been obtained in the critical regime where $\mu_k \lesssim T$. We have used the approximation $n_B(x) \simeq T/x$ for $|x| \leq T$, which is valid for $\mu_k \lesssim T$.

B. Conductivity in the critical regime

In order to complete the evaluation of the optical conductivity, we first notice that the summations over \mathbf{k} and \mathbf{k}' in Eqs. (4) and (5) vanish identically if Umklapp scattering is not taken into account (see Appendix A). Umklapp terms with $\mathbf{k}' = \mathbf{k} \pm n\mathbf{U}$, with \mathbf{U} being a reciprocal lattice wave vector, generate a finite result for the optical conductivity. This result is obtained by the scaling displayed in Eqs. (8)-(14) in the critical regime. In this regime, the second term $\chi_{J_{\mathbf{k}}^{(b)n_{\mathbf{k}}}}$ in Eq. (8) dominates over the first term (see Appendix B 2). Moreover, the MM evaluates to

$$M_{\mathbf{k}\mathbf{k}'}(\Omega_n) = \delta_{\mathbf{k}\mathbf{k}'} \frac{\lambda^4 T^2}{N^2 \Omega_n} \sum_{\omega_n, p_n} \sum_{\mathbf{p}, \mathbf{q}} D_{\mathbf{p}} D_{\mathbf{k}} D_{\mathbf{p}+\mathbf{q}} D_{\mathbf{k}+\mathbf{q}}, \quad (13)$$

which finally yields (see Appendix B 3)

$$M_{\mathbf{k}\mathbf{k}'}(\Omega) = \frac{\delta_{\mathbf{k}\mathbf{k}'} \lambda^4}{N^2} \frac{T^3}{192\pi^3 \mu_k^3} \left(\frac{\mu_k T}{\mu_k^2 + T^2} + \tanh^{-1} \frac{T}{\mu_k} \right). \quad (14)$$

Lastly, the optical conductivity can be rewritten as

$$\sigma(\Omega) = \sum_{\mathbf{k}} \frac{\chi_{\mathbf{k}\mathbf{k}}}{\chi_{\mathbf{k}\mathbf{k}}^{-1} M_{\mathbf{k}\mathbf{k}}(\Omega) - i\Omega}. \quad (15)$$

Noticing that the typical scaling relation $\mu_k \sim T$ holds in the critical regime (because T is the only energy scale in the problem and thus $k^2 \sim T$), the summation over \mathbf{k} in Eq. (15) can be finally performed. Scalings arguments lead to $\sum_{\mathbf{k}} \sim T$, $M_{\mathbf{k}\mathbf{k}} \sim T^0$, $\chi_{\mathbf{k}\mathbf{k}} \sim T^{-1}$, which result in a typical form for the optical conductivity given by

$$\sigma(\Omega) \sim \frac{1}{T - i\Omega}. \quad (16)$$

The aforementioned result has been further validated in the dc limit by numerically summing over \mathbf{k} in Eq. (15), which confirms our results in Ref. [32].

C. Lorenz ratio in the critical regime

The Wiedemann-Franz law [53] for the Lorenz ratio $L = \frac{\kappa}{\sigma T}$ is one of the most fundamental properties of a Fermi liq-

uid. It states that at low temperatures

$$\lim_{T \rightarrow 0} L = \frac{\pi^2}{3} \equiv L_0, \quad (17)$$

in units with $k_B = e = 1$. It reflects the fact that energy and charge are carried by the same degrees of freedom. To compute this ratio, we compute the thermal conductivity κ using the same method with the following substitution of the susceptibility $\chi_{J_{\mathbf{k}}^{(b)n_{\mathbf{k}}}} = \epsilon_{\mathbf{k}} \chi_{J_{\mathbf{k}} n_{\mathbf{k}}}$. At the critical regime, we get within the MM approach

$$\kappa(\Omega) = \frac{1}{T} \sum_{\mathbf{k}} \epsilon_{\mathbf{k}}^2 \frac{\chi_{\mathbf{k}\mathbf{k}}}{\chi_{\mathbf{k}\mathbf{k}}^{-1} M_{\mathbf{k}\mathbf{k}}(\Omega) - i\Omega}. \quad (18)$$

Scaling arguments lead to $\epsilon_{\mathbf{k}} \sim T$, which finally gives for the thermal conductivity

$$\kappa(\Omega) \sim \frac{T}{T - i\Omega}. \quad (19)$$

In the critical regime, the incoherent boson system obeys the correct scaling, $\frac{\kappa}{\sigma T} \sim C$, with C being a constant as $T \rightarrow 0$. However, although the Lorenz ratio is a constant, it does not satisfy the WF law because the coefficient is strongly dependent on the boson-boson coupling $\frac{\lambda^2}{2N}$ (as shown in Fig. 2) and so is model-dependent. This result is also confirmed using Kubo linear response in Appendix C. In the $t - J$ model [54] and near heavy fermion quantum critical point [55], stronger violations have been observed, where the Lorenz ratio does not saturate to a constant at low temperatures.

In the cuprates, the experimental situation is similar to our findings. The Lorenz ratio is found to saturate to a constant, both in the overdoped [14, 15, 56, 57] and underdoped [58] regimes, but the value of this constant depends on the oxygen doping. This experimental fact thus constrains the bosonic coupling λ of our model. We point out that this result can also be traced to the fact that we considered Umklapp scattering as the sole mechanism for momentum relaxation in the present calculation.

IV. CONCLUSIONS

In this paper, we have computed the transport properties of an effective model when charged fluctuating bosons (charge-two particle-particle bosons in this special case) are present at high energies in the phase diagram of the cuprate superconductors. The main results are as follows:

- A regime with approximately T -linear resistivity is obtained from the transport properties of the boson-fermion ‘‘soup’’. The charged bosons scatter with the fermions and become overdamped via the Landau damping $-i\gamma\omega$ (where ω is the real frequency). Optical conductivity was also evaluated [32] and yields a Drude-like conductivity for $\omega < T$ with a lifetime given by $\tau_{xx} = \tau_b \sim T^{-1}$. This agrees with experimental observation [59].

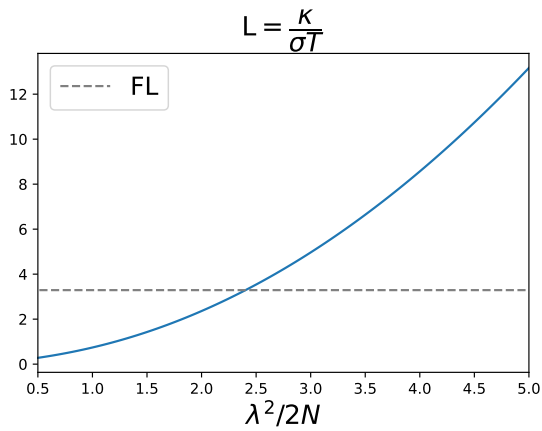


FIG. 2. The Lorenz ratio $L = \kappa/(\sigma T)$ (in units with $k_B = e = 1$) as a function of the bosonic coupling $g = \frac{\lambda^2}{2N}$, computed within the Kubo formalism. The same results are obtained with the memory matrix formalism. T is fixed such that it satisfies $T > \frac{\mu_0}{g}$, in order to be in the critical regime for all coupling values used.

- At low temperatures, the boson transport in the conductivity is “short-circuited” by the fermions that possess a transport lifetime $\tau_f \sim T^{-2}$. Hence, the regime where the bosons dominate the conductivity has a finite temperature range, which needs to be compared with the experimental data (this will be performed below).
- Due to the particle-hole symmetry of the Landau damped bosons, those charged bosons do not contribute to the Hall conductivity. This finding was already part of our previous study [32] and is also in good agreement with the experimental study of Ref. [26]. Therefore, the fermions dominate the Hall conductivity via hot-spot and cold-spot physics. A similar situation was studied in [35], where a linear-in- T longitudinal resistivity was assumed in parallel with “hot spot” and “cold spot” physics to estimate the Hall conductivity. Remarkably, their phenomenological analysis agreed with the experimental data and showed that the averaging around the Fermi surface for the Hall conductivity integral was weighting the hot spots more than for the longitudinal conductivity. A simplified understanding of their results in terms of a “lifetime picture” would give for the Hall conductivity from the fermions described by $\tau_{xy} \sim T^{-3/2}$, since the Hall average around the Fermi surface scans at the same time both the hot and cold regions. Altogether, in this regime, the cotangent of the Hall angle goes as $\cot \theta_H \sim \tau_{xx}/\tau_{xy}^2 \sim T^3/T \sim T^2$, which corresponds to the experimental observation.
- The thermal transport has also been calculated, and in the regime analyzed here (i.e., the critical case), the strict Wiedemann-Franz law (with the universal coefficient from the Fermi liquid theory) is violated at low temperatures due to the dependence on the bosonic coupling. In other words, although the Lorenz ratio does

converge to a constant at low temperatures, the WF law is violated in view of its dependence on the bosonic coupling. By constraining this coupling, the WF law can be brought to agree with recent experimental data [15], but as mentioned in the main text, there is still room for improvement here. It would be interesting to investigate also the effects of adding disorder via spatially random interactions in our model.

Finally, we point out that although our present study might not yet be the final solution for the strange metal phase of the cuprates, this perspective opens a new viewpoint on the physics of those compounds. The main idea is that at high energy scales, due to the strong superexchange interaction which brings the system to the regime of strong coupling, bosons of charge-zero (particle-hole) and charge-two (particle-particle) with a spectrum of wavevectors are generated. When the temperature is lowered, some of those bosons condense at a specific wave vector, giving rise to various orders, like, e.g., charge modulations or stripe physics depending on the compounds. Some bosons are unstable, like the charge-two finite vector ones related, e.g., to pair-density wave (PDW) order. In a recent line of ideas [16, 60, 61], the instability of the finite momentum charge-two bosons could be described by a theory of “fractionalization.” in which these excitations become entangled, opening a gap in the antinodal region of the Brillouin zone. In the strange metal phase, they also give rise to the regime of T -linear resistivity described in the present paper.

As mentioned above, it is worth plugging numbers to determine the possible boundaries of the obtained strange metal regime, which is valid above $T > T_{min}$. We point out that the constraint on T_{min} is such that the fermions should short-circuit the bosons for $T < T_{min}$. So we may impose that, for $T \lesssim T_{min}$, we have that $\sigma_f \gtrsim \sigma_b$. For a rough estimate, we can then use for the fermions that $\sigma_f = ne^2\tau_f/m_f^*$, where m_f^* is the quasiparticle effective mass. For the bosons, since we showed by means of scaling arguments within the MM formalism here and also using Kubo formalism in Ref. [32] that they also obey the Drude form for the conductivity, we have that $\sigma_b = n_b(2e)^2\tau_b/m_b$, where m_b is the mass introduced in Eq. (1). From Fig. 2 of Ref. [35], one obtains that $\sigma_f^{-1} = AT^2$, with $A \simeq 5 \cdot 10^{-3} \mu\Omega \cdot \text{cm}$. Thus, the reasonable range allowed experimentally for T_{min} is $1 \text{ K} < T_{min} < 10 \text{ K}$. If $T_{min} = 1 \text{ K}$, one would get $m_b/m_f^* \sim 0.02$, whereas if $T_{min} = 10 \text{ K}$ the ratio of masses should be given by $m_b/m_f^* \sim 0.2$. Given the strong mass renormalization of the fermions inside the strange metal phase of the present model, this range of the ratio of masses is conceivable in order to allow for a wide fluctuation regime where the incoherent bosons dominate the transport properties with respect to the fermions in the context of the resistivity of this non-Fermi liquid phase.

ACKNOWLEDGMENTS

We are grateful for discussion with G. Grissonnanche, N. Hussey, B. Ramshaw, L. Taillefer on various experimental is-

sues. H.F. acknowledges funding from CNPq under Grant No. 311428/2021-5. A.B. acknowledges support from the Kreitman School of Advanced Graduate Studies and European Research Council (ERC) Grant Agreement No. 951541, ARO (W911NF-20-1-0013).

Appendix A: Diagram contractions

We define the vertices as follows

$$V_{\mathbf{k},\mathbf{q},\mathbf{p}}^a = (2i\lambda^2) \begin{array}{c} k \\ \downarrow \\ p \rightsquigarrow \text{---} \text{---} \text{---} p+q \\ \downarrow \\ k+q \end{array}$$

$$V_{\mathbf{k},\mathbf{q},\mathbf{p}}^b = (2i\lambda^2) \begin{array}{c} k-q \\ \downarrow \\ p \rightsquigarrow \text{---} \text{---} \text{---} p+q \\ \downarrow \\ k \end{array}$$

and their conjugate counterpart. The vertices write

$$V_{\mathbf{k}} = \sum_{\mathbf{p},\mathbf{q}} V_{\mathbf{k},\mathbf{p},\mathbf{q}}, \quad (\text{A1})$$

$$\text{with } V_{\mathbf{k},\mathbf{p},\mathbf{q}} = V_{\mathbf{k},\mathbf{p},\mathbf{q}}^a - V_{\mathbf{k},\mathbf{p},\mathbf{q}}^b - h.c..$$

We construct the function $\mathcal{M}_{\mathbf{k},\mathbf{p},\mathbf{q}}$ by contracting

$$\begin{aligned} \mathcal{M}_{\mathbf{k},\mathbf{p},\mathbf{q}} &= \langle \bar{V}_{\mathbf{k},\mathbf{p},\mathbf{q}} \cdot \bar{V}_{\mathbf{k}',\mathbf{p}',\mathbf{q}'} \rangle, \\ &= \langle -V_{\mathbf{k},\mathbf{p},\mathbf{q}}^a \cdot V_{\mathbf{k}',\mathbf{p}',\mathbf{q}'}^a - V_{\mathbf{k},\mathbf{p},\mathbf{q}}^b \cdot V_{\mathbf{k}',\mathbf{p}',\mathbf{q}'}^b \\ &\quad + \bar{V}_{\mathbf{k},\mathbf{p},\mathbf{q}}^a \cdot V_{\mathbf{k}',\mathbf{p}',\mathbf{q}'}^a + \bar{V}_{\mathbf{k},\mathbf{p},\mathbf{q}}^b \cdot V_{\mathbf{k}',\mathbf{p}',\mathbf{q}'}^b \\ &\quad + V_{\mathbf{k},\mathbf{p},\mathbf{q}}^a \cdot V_{\mathbf{k}',\mathbf{p}',\mathbf{q}'}^b + V_{\mathbf{k},\mathbf{p},\mathbf{q}}^b \cdot V_{\mathbf{k}',\mathbf{p}',\mathbf{q}'}^a \\ &\quad - \bar{V}_{\mathbf{k},\mathbf{p},\mathbf{q}}^a \cdot V_{\mathbf{k}',\mathbf{p}',\mathbf{q}'}^b - \bar{V}_{\mathbf{k},\mathbf{p},\mathbf{q}}^b \cdot V_{\mathbf{k}',\mathbf{p}',\mathbf{q}'}^a + h.c. \rangle. \end{aligned} \quad (\text{A2})$$

There are eight types of contractions

$$\begin{aligned} 1) \langle V_{\mathbf{k},\mathbf{p},\mathbf{q}}^a \cdot V_{\mathbf{k}',\mathbf{p}',\mathbf{q}'}^a \rangle &= \delta_{\mathbf{k},\mathbf{k}'-\mathbf{q}} \delta_{\mathbf{p}',\mathbf{p}+\mathbf{q}} \delta_{\mathbf{q}',-\mathbf{q}} \mathcal{M}_{\mathbf{k},\mathbf{p},\mathbf{q}}, \\ 2) \langle V_{\mathbf{k},\mathbf{p},\mathbf{q}}^b \cdot V_{\mathbf{k}',\mathbf{p}',\mathbf{q}'}^b \rangle &= \delta_{\mathbf{k},\mathbf{k}'+\mathbf{q}} \delta_{\mathbf{p}',\mathbf{p}+\mathbf{q}} \delta_{\mathbf{q}',-\mathbf{q}} \mathcal{M}_{\mathbf{k},\mathbf{p},\mathbf{q}}, \\ 3) \langle V_{\mathbf{k},\mathbf{p},\mathbf{q}}^a \cdot V_{\mathbf{k}',\mathbf{p}',\mathbf{q}'}^b \rangle &= \delta_{\mathbf{k},\mathbf{k}'} \delta_{\mathbf{p}',\mathbf{p}+\mathbf{q}} \delta_{\mathbf{q}',-\mathbf{q}} \mathcal{M}_{\mathbf{k},\mathbf{p},\mathbf{q}}, \\ 4) \langle V_{\mathbf{k},\mathbf{p},\mathbf{q}}^b \cdot V_{\mathbf{k}',\mathbf{p}',\mathbf{q}'}^a \rangle &= \langle V_{\mathbf{k},\mathbf{p},\mathbf{q}}^a \cdot V_{\mathbf{k}',\mathbf{p}',\mathbf{q}'}^b \rangle, \\ 5) \langle \bar{V}_{\mathbf{k},\mathbf{p},\mathbf{q}}^a \cdot V_{\mathbf{k}',\mathbf{p}',\mathbf{q}'}^a \rangle &= \delta_{\mathbf{k},\mathbf{k}'} \delta_{\mathbf{p}',\mathbf{p}} \delta_{\mathbf{q}',\mathbf{q}} \mathcal{M}_{\mathbf{k},\mathbf{p},\mathbf{q}}, \\ 6) \langle \bar{V}_{\mathbf{k},\mathbf{p},\mathbf{q}}^b \cdot V_{\mathbf{k}',\mathbf{p}',\mathbf{q}'}^b \rangle &= \langle \bar{V}_{\mathbf{k},\mathbf{p},\mathbf{q}}^a \cdot V_{\mathbf{k}',\mathbf{p}',\mathbf{q}'}^a \rangle, \\ 7) \langle \bar{V}_{\mathbf{k},\mathbf{p},\mathbf{q}}^a \cdot V_{\mathbf{k}',\mathbf{p}',\mathbf{q}'}^b \rangle &= \delta_{\mathbf{k},\mathbf{k}'-\mathbf{q}} \delta_{\mathbf{p}',\mathbf{p}+\mathbf{q}} \delta_{\mathbf{q}',\mathbf{q}} \mathcal{M}_{\mathbf{k},\mathbf{p},\mathbf{q}}, \\ 8) \langle \bar{V}_{\mathbf{k},\mathbf{p},\mathbf{q}}^b \cdot V_{\mathbf{k}',\mathbf{p}',\mathbf{q}'}^a \rangle &= \delta_{\mathbf{k},\mathbf{k}'+\mathbf{q}} \delta_{\mathbf{p}',\mathbf{p}+\mathbf{q}} \delta_{\mathbf{q}',\mathbf{q}} \mathcal{M}_{\mathbf{k},\mathbf{p},\mathbf{q}}. \end{aligned} \quad (\text{A3})$$

Altogether, we finally have

$$M_{\mathbf{k}\mathbf{k}'}(\Omega) = 4 \sum_{\mathbf{p},\mathbf{q}} (\delta_{\mathbf{k},\mathbf{k}'} - \delta_{\mathbf{k},\mathbf{k}'\pm\mathbf{q}}) \mathcal{M}_{\mathbf{k},\mathbf{p},\mathbf{q}}, \quad (\text{A4})$$

which vanishes if Umklapp scattering is not taken into account. Umklapp terms provide a nonzero value to $M_{\mathbf{k}\mathbf{k}'}(\Omega)$, leading to Eq. (14) presented in the main part of the manuscript.

Appendix B: Evaluations

1. Susceptibilities

After performing a spectral decomposition of the boson Green's function Eq. (7), the first part of the susceptibility $\chi_{J_{\mathbf{k}}n_{\mathbf{k}}}$ writes

$$\begin{aligned} \chi_{J_{\mathbf{k}}n_{\mathbf{k}}}^{(a)} &= \mathbf{v}_{\mathbf{k}} \int_{-D}^D \frac{dE}{2\pi} n_B(E) \frac{E}{E^2 + \mu_{\mathbf{k}}^2} \\ &= \mathbf{v}_{\mathbf{k}} \frac{n_B(\mu_{\mathbf{k}})}{\pi} \ln \left(\frac{D}{\mu_{\mathbf{k}}} \right), \end{aligned} \quad (\text{B1})$$

with the convention $n_B(E) = \exp \delta E / (\exp \beta E - 1)$, with $\delta \ll 1$ being a regulator for negative energies.

As for the susceptibility $\chi_{\mathbf{k}\mathbf{k}}$, we proceed in the same way with a spectral decomposition of each boson propagator given by

$$\begin{aligned} \chi_{\mathbf{k}\mathbf{k}} &= \int \frac{dE_1 dE_2}{(2\pi)^2} \frac{n_B(E_1) - n_B(E_2)}{-E_1 + E_2} \frac{E_1}{E_1^2 + \mu_{\mathbf{k}}^2} \frac{E_2}{E_2^2 + \mu_{\mathbf{k}}^2} \\ &= \int_0^T \frac{dE_1 dE_2}{(2\pi)^2} \frac{T}{(E_1^2 + \mu_{\mathbf{k}}^2)(E_2^2 + \mu_{\mathbf{k}}^2)} \\ &= \frac{T}{\mu_{\mathbf{k}}^2} \left(\tanh^{-1} \frac{T}{\mu_{\mathbf{k}}} \right)^2, \end{aligned} \quad (\text{B2})$$

where in the second line we have used the approximation $n_B(x) \simeq T/x$ for $|x| \leq T$, which is valid for $\mu_{\mathbf{k}} \lesssim T$.

2. Remarks on the scaling of the optical conductivity

In the scaling of the optical conductivity of Eq. (4), the two terms $\chi_{J_{\mathbf{k}}n_{\mathbf{k}}}^{(a)}$ and $\chi_{J_{\mathbf{k}}n_{\mathbf{k}}}^{(b)}$ behave differently. Any term proportional to $\chi_{J_{\mathbf{k}}n_{\mathbf{k}}}^{(a)}$ in the summation over the momentum in Eq. (4) gives a UV divergence (after turning the summation over the momentum into an integral in the thermodynamic limit). In other words, the typical momentum of the integral is such that $\mu_{\mathbf{k}} \sim D$, where D is the bandwidth. Then, the factor $n_B(\mu_{\mathbf{k}}) \sim n_B(D)$ in Eq. (8) leads to an exponentially small contribution. On the other hand, the contribution related to $\chi_{J_{\mathbf{k}}n_{\mathbf{k}}}^{(b)}$ in the optical conductivity integral in Eq. (4) is dominated by a typical momentum such that $\mu_{\mathbf{k}} \sim T$. This leads to the result of Eq. (16).

3. Memory Matrix

The MM, after spectral decomposition, writes

$$M_{\mathbf{k}\mathbf{k}}(\Omega_n) = \frac{\lambda^4}{N^2} \frac{1}{\Omega_n} T \sum_{\omega_q} \sum_{\mathbf{p}, \mathbf{q}} \int \prod_{i=1}^4 \frac{dE_i}{2\pi} F(E_i) \times \frac{n_B(E_3) - n_B(E_4)}{E_3 - E_4 + i\omega_q} \frac{n_B(E_1) - n_B(E_2)}{E_1 - E_2 + i\omega_q + i\Omega_n}, \quad (\text{B3})$$

with $F(E) = \frac{E}{E^2 + \mu_k^2}$. Performing the sum over ω_q , we get

$$M_{\mathbf{k}\mathbf{k}}(\Omega_n) = \frac{\lambda^4}{N^2} \frac{1}{\Omega_n} \sum_{\mathbf{p}, \mathbf{q}} \int \prod_{i=1}^4 \frac{dE_i}{2\pi} F(E_i) \times [n_B(E_1) - n_B(E_2)] [n_B(E_3) - n_B(E_4)] \times \frac{n_B(E_1 - E_2) - n_B(E_3 - E_4)}{E_1 - E_2 - E_3 + E_4 + i\Omega_n}. \quad (\text{B4})$$

We now perform analytic continuation $i\Omega_n \rightarrow \Omega + i\delta$. We obtain, after taking the limit $\Omega \rightarrow 0$,

$$M_{\mathbf{k}\mathbf{k}}(\Omega) = \frac{\lambda^4}{N^2} \pi \sum_{\mathbf{p}, \mathbf{q}} \int \prod_{i=1}^4 \frac{dE_i}{2\pi} F(E_i) \times [n_B(E_1) - n_B(E_2)] [n_B(E_3) - n_B(E_4)] \times \delta(E_1 - E_2 - E_3 + E_4) \left. \frac{\partial n_B}{\partial E} \right|_{E_1 - E_2}. \quad (\text{B5})$$

We now use $\partial n_B / \partial E \simeq -T/E^2$, if $|E| < T$ and zero elsewhere. We have a factor $-T/(E_1 - E_2)^2$, with the condition that $|E_1 - E_2| < T$. We thus have $E_2 \simeq E_1 \pm T$ and form resolving the δ -function, $E_4 \simeq E_3 \pm T$. This in turn gives $n_B(E_1) - n_B(E_2) \simeq (\partial n_B / \partial E_1) T \simeq -T^2/E_1^2$ and likewise $n_B(E_3) - n_B(E_4) \simeq -T^2/E_3^2$. Eliminating two variables in the integral Eq. (B5), but remembering that $|E_1 - E_2| < T$ and $|E_3 - E_4| < T$, leads to

$$M_{\mathbf{k}\mathbf{k}}(\Omega) = \frac{\lambda^4}{N^2} \frac{\pi}{(2\pi)^4} \sum_{\mathbf{p}, \mathbf{q}} \int_{-T}^T \int_{-T}^T dE_1 dE_3 T^4 \times \frac{1}{(E_1^2 + \mu_p^2)(E_1^2 + \mu_{p+q}^2)(E_3^2 + \mu_k^2)(E_3^2 + \mu_{k+q}^2)} = \frac{\lambda^4}{N^2} \frac{\pi}{(2\pi)^4} T^4 \sum_{\mathbf{p}, \mathbf{q}} I_{\mathbf{p}, \mathbf{q}} I_{\mathbf{k}, \mathbf{q}}. \quad (\text{B6})$$

With $(a, b) = (\mu_p, \mu_{p+q})$ for the first integral and $(a, b) = (\mu_k, \mu_{k+q})$ for the second integral, we obtain the following result

$$I_{a,b} = 2 \int_0^T \frac{dx}{(x^2 + a^2)(x^2 + b^2)} = 2 \left[\frac{-b \tan^{-1} \frac{T}{a} + a \tan^{-1} \frac{T}{b}}{ab(a^2 - b^2)} \right]. \quad (\text{B7})$$

In order to go further, we need to perform the integration over \mathbf{p} and \mathbf{q} . For this reason, we assume (and this can be also checked at the end of the calculation) that the order of magnitude of the various wave vectors is such that they are all scaling with temperature as $k \sim q \sim p \sim \sqrt{T}$. We can thus use $\mu_{k+q} \simeq \mu_k$ inside the integrals. We then have

$$M_{\mathbf{k}\mathbf{k}}(\Omega) = \frac{\lambda^4}{N^2} \frac{\pi}{(2\pi)^4} T^4 J_{\mathbf{p}, \mathbf{q}} \frac{1}{\mu_k^3} \left[\frac{\mu_k T}{\mu_k^2 + T^2} + \tan^{-1} \frac{T}{\mu_k} \right], \quad (\text{B8})$$

with

$$J_{\mathbf{p}, \mathbf{q}} = \int_0^T \int_0^T \frac{dp^2 dq^2}{(\mu_p^2 - \mu_{p+q}^2)} \left[-\frac{1}{\mu_{p+q}} \tan^{-1} \frac{T}{\mu_p} + \frac{1}{\mu_p} \tan^{-1} \frac{T}{\mu_{p+q}} \right]. \quad (\text{B9})$$

Recalling that $\mu_p = p^2 + T$ and $\mu_{p+q} = (p+q)^2 + T$, and expanding $\tan^{-1}(T/\mu_p) \sim T/\mu_p - (T/\mu_p)^3$, we get

$$J_{\mathbf{p}, \mathbf{q}} \simeq \frac{T^3}{3} \int_0^T \frac{dp^2 d(p+q)^2}{\mu_p^3 \mu_{p+q}^3} = \frac{1}{12T}. \quad (\text{B10})$$

Putting together Eqs. (B8) and (B10), it leads to

$$M_{\mathbf{k}\mathbf{k}}(\Omega) = \frac{\lambda^4}{N^2} \frac{\pi}{12} \frac{T^3}{(2\pi)^4} \frac{1}{\mu_k^3} \left(\frac{\mu_k T}{\mu_k^2 + T^2} + \tanh^{-1} \frac{T}{\mu_k} \right), \quad (\text{B11})$$

which is the result presented in the main part of the manuscript.

Appendix C: Comparison with Kubo formalism

Here, we compare the results obtained within the memory matrix formalism with the standard Kubo formalism [62]. Following our previous work [32], the optical conductivity and the thermal conductivity (as we pointed out in the main text, the thermal conductivity at zero electric field $\bar{\kappa}$ and the thermal conductivity at zero electric current κ are equal in the present calculation) are given, respectively, by

$$\sigma(\omega) = -\frac{\mathcal{K}_0(\omega_n)}{\omega_n} \Big|_{i\omega_n \rightarrow \omega + i0^+}, \quad (\text{C1})$$

$$\kappa(\omega) = -\frac{1}{T} \frac{\mathcal{K}_2(\omega_n)}{\omega_n} \Big|_{i\omega_n \rightarrow \omega + i0^+}, \quad (\text{C2})$$

with \mathcal{K}_α computed using the spectral decomposition of the boson propagator $D^{-1}(\mathbf{q}, \omega_n) = |\omega_n| + \mu_{\mathbf{q}}(T)$ used in Eq. (B1)

$$\mathcal{K}_\alpha(\omega_n) = -\sum_{\mathbf{q}} \epsilon_{\mathbf{q}}^\alpha \int \frac{dE_1 dE_2}{(2\pi)^2} \frac{n_B(E_1) - n_B(E_2)}{-E_1 + E_2 + \omega_n} \frac{E_1}{E_1^2 + \mu_{\mathbf{q}}^2} \frac{E_2}{E_2^2 + \mu_{\mathbf{q}}^2}. \quad (\text{C3})$$

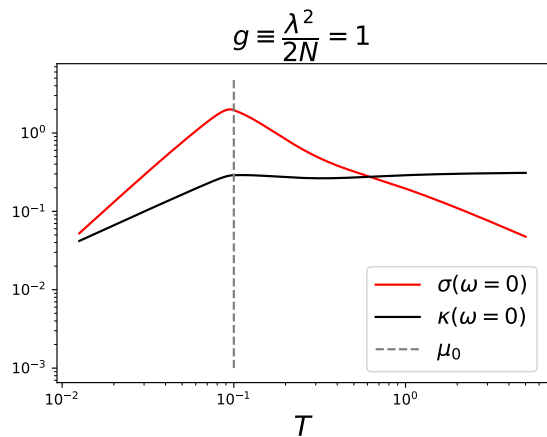


FIG. 3. The electrical conductivity and thermal conductivity as a function of T computed within Kubo formalism in units with $e = 1$ and $\hbar = 1$. Here, we set $g \equiv \frac{\lambda^2}{2N} = 1$. For $T > \mu_0$, in the critical regime, the constant behavior of κ and the $\frac{1}{T}$ behavior of σ set in.

Performing an analytical continuation $\omega_n \rightarrow \omega + i\delta$ and considering the limit $\omega \rightarrow 0$, we get:

$$\mathcal{K}_\alpha(\omega) = \frac{T\omega}{4\pi} \sum_{\mathbf{q}} \epsilon_{\mathbf{q}}^\alpha \int \frac{dE}{(2\pi)^2} \frac{T}{E^2} \left(\frac{E}{E^2 + \mu_{\mathbf{q}}^2} \right)^2. \quad (\text{C4})$$

\mathcal{K}_α can be integrated explicitly and we obtain the optical and thermal conductivities σ and κ shown in Fig. 3.

The T -dependence of μ is given by

$$\mu \equiv \mu(T) = \begin{cases} \mu_0 + \frac{\lambda^2}{2N} T \ln\left(\frac{T}{\mu_0}\right) & \text{for } T \gg \mu_0, \\ \mu_0 & \text{for } T \ll \mu_0. \end{cases} \quad (\text{C5})$$

We consider the critical regime to compare our results with those obtained from the memory matrix formalism. T satisfies $T > \mu_0$ and $T > \frac{\lambda^2 \mu_0}{2N}$; thus, we can approximate $\frac{\mu}{T} \approx \frac{\lambda^2}{2N}$ by neglecting logarithmic corrections. In this regime, we have $\sigma = \frac{1}{T} \tilde{\sigma}(\mu/T)$ and $\kappa = \tilde{\kappa}(\mu/T)$, in agreement with the scaling obtained using the memory matrix formalism in the critical regime in Eqs. (16) and (19). If we consider logarithmic corrections in $\mu(T)$, the results obtained remain qualitatively similar up to a weak dependence on T .

In contrast to the Fermi liquid case, the Lorenz ratio $L = \frac{\kappa}{\sigma T} = \frac{\tilde{\kappa}}{\tilde{\sigma}}$ is not given by a universal constant but depends on the interaction strength $g = \frac{\lambda^2}{2N}$. This is due to the infrared (IR) dependence on the integration over \mathbf{q} for the optical conductivity. Because the integral is divergent, it explicitly depends on the IR cutoff which is μ/T , and leads to the g -dependence of L . The Lorenz ratio increases with the bosonic coupling in this regime, as shown in Fig. 2.

-
- [1] B. Keimer, S. A. Kivelson, M. R. Norman, S. Uchida, and J. Zaanen, *Nature* **518**, 179 (2015).
- [2] M. R. Norman and C. Pépin, *Rep. Prog. Phys.* **66**, 1547 (2003).
- [3] P. A. Lee, N. Nagaosa, and X.-G. Wen, *Rev. Mod. Phys.* **78**, 17 (2006).
- [4] M. Gurvitch and A. T. Fiory, *Phys. Rev. Lett.* **59**, 1337 (1987).
- [5] V. J. Emery and S. A. Kivelson, *Phys. Rev. Lett.* **74**, 3253 (1995).
- [6] N. Hussey, K. Takenaka, and H. Takagi, *Philosophical Magazine* **84**, 2847 (2004).
- [7] A. Legros, S. Benhabib, W. Tabis, F. Laliberté, M. Dion, M. Lizaire, B. Vignolle, D. Vignolles, H. Raffy, Z. Z. Li, P. Auban-Senzier, N. Doiron-Leyraud, P. Fournier, D. Colson, L. Taillefer, and C. Proust, *Nature Physics* **15**, 142 (2018).
- [8] J. Clayhold, N. P. Ong, Z. Z. Wang, J. M. Tarascon, and P. Barboux, *Physical Review B* **39**, 7324 (1989).
- [9] Y. Ando and T. Murayama, *Phys. Rev. B* **60**, R6991 (1999).
- [10] N. Barišić, M. Chan, M. Veit, C. Dorow, Y. Ge, Y. Li, W. Tabis, Y. Tang, G. Yu, X. Zhao, *et al.*, *New Journal of Physics* **21**, 113007 (2019).
- [11] P. Coleman, A. J. Schofield, and A. M. Tsvelik, *Journal of Physics: Condensed Matter* **8**, 9985 (1996).
- [12] C. M. Varma, P. B. Littlewood, S. Schmitt-Rink, E. Abrahams, and A. E. Ruckenstein, *Phys. Rev. Lett.* **63**, 1996 (1989).
- [13] E. Abrahams and C. M. Varma, *Phys. Rev. B* **68**, 094502 (2003).
- [14] C. Proust, E. Boaknin, R. W. Hill, L. Taillefer, and A. P. Mackenzie, *Phys. Rev. Lett.* **89**, 147003 (2002).
- [15] B. Michon, A. Ataie, P. Bourgeois-Hope, C. Collignon, S. Y. Li, S. Badoux, A. Gourgout, F. Laliberté, J.-S. Zhou, N. Doiron-Leyraud, and L. Taillefer, *Phys. Rev. X* **8**, 041010 (2018).
- [16] G. Grissonnanche, F. Laliberté, S. Dufour-Beauséjour, M. Matusiak, S. Badoux, F. F. Tafti, B. Michon, A. Riopel, O. Cyr-Choynière, J. C. Baglo, B. J. Ramshaw, R. Liang, D. A. Bonn, W. N. Hardy, S. Krämer, D. LeBoeuf, D. Graf, N. Doiron-Leyraud, and L. Taillefer, *Phys. Rev. B* **93**, 064513 (2016).
- [17] A. A. Patel and S. Sachdev, *Phys. Rev. B* **90**, 165146 (2014).
- [18] A. A. Patel, J. McGreevy, D. P. Arovas, and S. Sachdev, *Phys. Rev. X* **8**, 021049 (2018).
- [19] J. Zaanen, *SciPost Phys.* **6**, 061 (2019).
- [20] A. Abanov and A. V. Chubukov, *Phys. Rev. Lett.* **84**, 5608 (2000).
- [21] R. Hlubina and T. M. Rice, *Phys. Rev. B* **51**, 9253 (1995).
- [22] A. Rosch, *Phys. Rev. Lett.* **82**, 4280 (1999).
- [23] X. Wang and E. Berg, *Phys. Rev. B* **99**, 235136 (2019).
- [24] D. Chowdhury, A. Georges, O. Parcollet, and S. Sachdev, *Rev. Mod. Phys.* **94**, 035004 (2022).
- [25] L. V. Delacrétaz, B. Goutéraux, S. A. Hartnoll, and A. Karlsson, *SciPost Phys.* **3**, 025 (2017).
- [26] C. Putzke, S. Benhabib, W. Tabis, J. Ayres, Z. Wang, L. Malone, S. Licciardello, J. Lu, T. Kondo, T. Takeuchi, N. E. Hussey, J. R. Cooper, and A. Carrington, *Nature Physics* **17**, 826 (2021).
- [27] I. Bozovic, G. Logvenov, M. A. J. Verhoeven, P. Caputo, E. Goldobin, and M. R. Beasley, *Phys. Rev. Lett.* **93**, 157002 (2004).
- [28] S. Caprara, C. Di Castro, G. Seibold, and M. Grilli, *Phys. Rev. B* **95**, 224511 (2017).

- [29] K. B. Efetov, H. Meier, and C. Pépin, *Nat. Phys.* **9**, 442 (2013).
- [30] H. Kontani, *Reports on Progress in Physics* **71**, 026501 (2008).
- [31] J. Merino and R. H. McKenzie, *Phys. Rev. B* **61**, 7996 (2000).
- [32] A. Banerjee, M. Grandadam, H. Freire, and C. Pépin, *Phys. Rev. B* **104**, 054513 (2021).
- [33] C. Pépin and H. Freire, *Annals of Physics*, 169233 (2023).
- [34] C. Yang, H. Liu, Y. Liu, J. Wang, D. Qiu, S. Wang, Y. Wang, Q. He, X. Li, P. Li, Y. Tang, J. Wang, X. C. Xie, J. M. Valles, J. Xiong, and Y. Li, *Nature* **601**, 205 (2022).
- [35] J. Kokalj, N. E. Hussey, and R. H. McKenzie, *Phys. Rev. B* **86**, 045132 (2012).
- [36] S. A. Hartnoll, A. Lucas, and S. Sachdev, *Holographic Quantum Matter* (MIT Press, Cambridge, 2018).
- [37] D. Forster, *Hydrodynamic Fluctuations, Broken Symmetry, and Correlation Functions* (W. A. Benjamin, Reading, 1975).
- [38] W. Götze and P. Wölfle, *Phys. Rev. B* **6**, 1226 (1972).
- [39] A. Rosch and N. Andrei, *Phys. Rev. Lett.* **85**, 1092 (2000).
- [40] R. Mahajan, M. Barkeshli, and S. A. Hartnoll, *Phys. Rev. B* **88**, 125107 (2013).
- [41] A. Lucas and S. Sachdev, *Phys. Rev. B* **91**, 195122 (2015).
- [42] S. A. Hartnoll, R. Mahajan, M. Punk, and S. Sachdev, *Phys. Rev. B* **89**, 155130 (2014).
- [43] L. E. Vieira, V. S. de Carvalho, and H. Freire, *Annals of Physics* **419**, 168230 (2020).
- [44] H. Freire, *Ann. Phys. (N. Y.)* **384**, 142 (2017).
- [45] H. Freire, *EPL (Europhysics Letters)* **118**, 57003 (2017).
- [46] H. Freire, *EPL (Europhysics Letters)* **124**, 27003 (2018).
- [47] H. Freire, *Ann. Phys. (N. Y.)* **349**, 357 (2014).
- [48] J. Zaanen, Y. Liu, Y.-W. Sun, and K. Schalm, *Holographic Duality in Condensed Matter Physics* (Cambridge University Press, Cambridge, 2015).
- [49] I. Mandal and H. Freire, *Phys. Rev. B* **103**, 195116 (2021).
- [50] H. Freire and I. Mandal, *Physics Letters A* **407**, 127470 (2021).
- [51] I. Mandal and H. Freire, *Journal of Physics: Condensed Matter* **34**, 275604 (2022).
- [52] X. Wang and E. Berg, *Phys. Rev. B* **105**, 045137 (2022).
- [53] G. Chester and A. Thellung, *Proceedings of the Physical Society (1958-1967)* **77**, 1005 (1961).
- [54] A. Houghton, S. Lee, and J. B. Marston, *Phys. Rev. B* **65**, 220503(R) (2002).
- [55] K.-S. Kim and C. Pépin, *Phys. Rev. Lett.* **102**, 156404 (2009).
- [56] C. Proust, E. Boaknin, R. W. Hill, L. Taillefer, and A. P. Mackenzie, *Phys. Rev. Lett.* **89**, 147003 (2002).
- [57] S. Nakamae, K. Behnia, N. Mangkorntong, M. Nohara, H. Takagi, S. J. C. Yates, and N. E. Hussey, *Phys. Rev. B* **68**, 100502(R) (2003).
- [58] G. Grissonnanche, F. Laliberté, S. Dufour-Beauséjour, M. Matusiak, S. Badoux, F. F. Tafti, B. Michon, A. Riopel, O. Cyr-Choynière, J. C. Baglo, B. J. Ramshaw, R. Liang, D. A. Bonn, W. N. Hardy, S. Krämer, D. LeBoeuf, D. Graf, N. Doiron-Leyraud, and L. Taillefer, *Phys. Rev. B* **93**, 064513 (2016).
- [59] B. Michon, C. Berthod, C. W. Rischau, A. Ataei, L. Chen, S. Komiyama, S. Ono, L. Taillefer, D. van der Marel, and A. Georges, *Nature Communications* **14**, 3033 (2023).
- [60] M. Grandadam, D. Chakraborty, and C. Pépin, *Journal of Superconductivity and Novel Magnetism* **33**, 2361 (2020).
- [61] A. Banerjee, A. Ferraz, and C. Pépin, *Phys. Rev. B* **106**, 024505 (2022).
- [62] R. Kubo, *Journal of the Physical Society of Japan* **12**, 570 (1957).